COMPUTER RESEARCH AND MODELING
2025 VOL. 17 NO. 4 P. 737–752
DOI: 10.20537/2076-7633-2025-17-4-737-752

Ки&М

ANALYSIS AND MODELING OF COMPLEX LIVING SYSTEMS

UDC: 51-76

Modeling the indirect impact of rhinoceros beetle control on red palm weevils in coconut plantations

B. Dhivyadharshini, R. Senthamarai[a]

Department of Mathematics, College of Engineering and Technology, SRM Institute of Science and Technology, Kattankulathur – 603 203, Tamil Nadu, India

E-mail: [a] senthamr@srmist.edu.in

Received 11.06.2025.
Accepted for publication 23.07.2025.

In this paper, a mathematical model is developed and analyzed to assess the indirect impact of controlling rhinoceros beetles on red palm weevil populations in coconut plantations. The model consists of a system of six non-linear ordinary differential equations (ODEs), capturing the interactions among healthy and infected coconut trees, rhinoceros beetles, red palm weevils, and the oryctes virus. The model ensures biological feasibility through positivity and boundedness analysis. The basic reproduction number R_0 is derived using the next-generation matrix method. Both local and global stability of the equilibrium points are analyzed to determine conditions for pest persistence or eradication. Sensitivity analysis identifies the most influential parameters for pest management. Numerical simulations reveal that by effectively controlling the rhinoceros beetle population particularly through infection with the oryctes virus, the spread of the red palm weevil can also be suppressed. This indirect control mechanism helps to protect the coconut tree population more efficiently and supports sustainable pest management in coconut plantations.

Keywords: mathematical modeling, coconut plantation dynamics, non-linear ordinary differential equations, pest control model, numerical simulation

Citation: *Computer Research and Modeling*, 2025, vol. 17, no. 4, pp. 737–752.

The authors are pleased to acknowledge the financial support of the Selective Excellence Research Initiative (SRMIST/R/AR(A)/SERI2023/174/31).

1. Introduction

Cocos nucifera, commonly referred to as the coconut tree, was a vital cultivated palm, providing benefits from its fruit to its trunk. Globally, India ranked as the third-largest producer of coconut and its by-products [Sreejith et al., 2013]. The livelihoods of families and industries reliant on the coconut economy were significantly affected by any disease that reduced coconut plantation yields. An inherent and crucial characteristic of coconut fruit was its antiviral properties [Varghese, Jacob, 2017]. As per research carried out by Dayrit, the coconut product market became the fastest-growing industry as a result of the anti-viral compounds that were present in it, which were shown to be effective in the treatment of COVID-19 [Dayrit, Mary, 2020]. In addition to vitamins C, E, B1, B3, B5, and B6, it contained minerals such as selenium, iron, calcium, magnesium, phosphorus, and salt [Ijinu et al., 2011]. September 2nd was designated as World Coconut Day by the members of the International Coconut Community (ICC), of which India was a founding member, to commemorate the production [Jayasekhar et al., 2019]. Indonesia, India, and the Philippines were the top coconut-producing countries. In India, major coconut-growing states like Kerala and Tamil Nadu used 50 % of production for food and religious purposes, 35 % for copra, 11 % for tender coconuts, and 2 % each for seeds and value-added products. Coconut was valued as a "functional food" for its health benefits [Nadanasabapathy, Kumar, 2013].

Oryctes rhinoceros, also known as coconut rhinoceros beetle (CRB), also called the Asiatic or coconut palm rhinoceros beetle, was a sizable insect measuring about 4 to 5 cm, and was a member of the Dynastinae subfamily known for attacking coconut and oil palms [Bedford, 1980; Bedford, 2013]. This beetle can inflict severe damage to young fronds, potentially leading to the death of the palm, and it typically bred in rotting palm trunks or organic materials such as sawdust and compost piles [Barlow, Chew, 1970]. The red palm weevil (Rhynchophorus ferrugineus) was a destructive pest that attacked coconut, date, and oil palms, causing severe agricultural losses. Native to Southeast Asia, its larvae burrowed into palm trunks, often going undetected until the tree was irreversibly damaged. Control methods included pheromone traps, biological agents, and insecticides, with early detection and integrated pest management being key to containment [Nair et al., 1998; Nirula et al., 1953]. Oryctes rhinoceros nudivirus (OrNV) was introduced in Pacific islands and successfully suppressed CRB populations, stopping their spread for three decades. However, outbreaks may resurfaced when breeding sites multiplied, particularly after cyclones or palm removal. Integrated pest management now utilized OrNV-based biocontrol alongside rigorous sanitation practices to effectively curb CRB outbreaks [Secretariat of the Pacific Community, 2015; Marshall et al., 2017].

The concept and formulation of epidemiological models were presented in [Allen et al., 2019], highlighting their importance in capturing the dynamics of interacting populations and enabling a clearer understanding of variable relationships and biological implications. Pest control played a crucial role in achieving high crop yields and maintaining plant health in agriculture. The analytical study of non-linear prey-predator systems was explored using the homotopy perturbation method (HPM) [Dhivyadharshini, Senthamarai, 2022]. Mathematical modeling was applied to investigate the invasion and control of the CRB in Guam, providing insights into its population dynamics [Caasia, Guerrerob, 2023]. Similarly, the infestation of rugose spiraling whitefly on coconut trees was analyzed using delay differential equations, with solutions approximated via HPM [Dhivyadharshini, Senthamarai, 2024]. Beyond ecological systems, deterministic and stochastic models were developed to examine the dynamics of drug-resistant tuberculosis, highlighting key factors influencing its spread [Umana et al., 2016]. In agricultural pest management, the role of awareness campaigns in controlling coconut tree pests was mathematically modeled, assessing their effectiveness in reducing infestations [Suganya, Senthamarai, 2022a]. Integrated pest management strategies for key coconut insect pests were studied, emphasizing sustainable control measures [Winotai, 2014]. Non-linear models for pest control in coconut trees were also analytically approximated using the homotopy analysis

method (HAM), offering precise solutions to complex dynamics [Suganya, Senthamarai, 2022a]. Molecular techniques were employed to evaluate the OrNV as a biological control agent in oil palm plantations, demonstrating its potential for beetle suppression [Moslim et al., 2011]. Mathematical modeling was utilized to analyze the impact of the rugose spiraling whitefly on coconut trees, providing a framework for understanding its ecological and economic consequences [Suganya, Senthamarai, 2022a]. While earlier studies [Caasia, Guerrerob, 2023; Hochberg, Waage, 1991] modeled the control of CRB, our work focused on how such control efforts influenced red palm weevil dynamics through indirect interactions in coconut plantations.

In this paper, we analyzed ODEs to manage indirect impact of CRB control on red palm weevils in coconut plantations. The dynamics of the model were analyzed using MATLAB software. The Pollachi area in Tamil Nadu served as the main focus for our study and guided the choice of parameter values. We assessed equilibrium point stability and determined the reproduction number via a next-generation matrix. Sensitivity analysis highlighted the parameters with the greatest effect on the system.

Section 2 introduces the ODE model, while Section 3 investigates the basic properties of the model, including equilibria and stability analysis. Section 4 addresses parameter sensitivity. Section 5 presents the results and discussion, and finally, Section 6 summarizes the key findings and conclusions of the study.

2. Mathematical formulation of the problem

Based on the assumptions and derivations presented below, the model is represented by a deterministic set of non-linear differential equations.

The tree density is classified into healthy trees H and infected trees X to evaluate the beetles effect on coconut trees. The rhinoceros beetle population is also classified into healthy R_H and infected beetles R_I, where the total beetle population is given by $R = R_H + R_I$. W refers to the population of red weevils, and Y indicates the number of OrNV carried out over the time period t.

The population of healthy coconut tree (H) is generated by the growth rate of healthy coconut trees s reduced by the attacks by the CRBs and red palm weevils with a holling type II functional response. Thus,

$$\frac{dH}{dt} = s - \left(\frac{\alpha_1 RH}{1+\gamma_1 H} + \frac{\alpha_2 WH}{1+\gamma_2 H}\right). \tag{1}$$

The population of infected coconut tree (X) is generated by the infection of trees by beetles and weevils, along with death rate of infected trees. Thus,

$$\frac{dX}{dt} = \left(\frac{\alpha_1 RH}{1+\gamma_1 H} + \frac{\alpha_2 WH}{1+\gamma_2 H}\right) - \left(k_1 R + k_2 W\right) X - rX. \tag{2}$$

The population of healthy rhinoceros beetles (R_H) is generated by the logistic growth of the healthy rhinoceros beetle population, its natural mortality, and infection by the oryctes virus. Thus,

$$\frac{dR_H}{dt} = \gamma_1 R_H \left(1 - \frac{R}{k_R}\right) - \mu_R R_H - \beta R_H R_I. \tag{3}$$

The population of infected rhinoceros beetles (R_I) is generated by its dynamics with infection, mortality, and virus-related death. Thus,

$$\frac{dR_I}{dt} = \beta R_H R_I - (\mu_R + \gamma Y) R_I. \tag{4}$$

The population of red weevil (W) is generated by the logistic growth of the red palm weevil population, natural death, and the effect of controlling CRBs on the weevil population. Thus,

$$\frac{dW}{dt} = \gamma_2 W\left(1 - \frac{W}{k_W}\right) - \mu_W W - \theta RW. \tag{5}$$

The population of oryctes virus (Y) is generated by the external contribution to virus growth, as it is spread by infected beetles and decays over time. Thus,

$$\frac{dY}{dt} = \delta_v + \rho R_I - \eta Y \tag{6}$$

with the following initial conditions:

$$\begin{gathered} H(0) = l > 0, \quad X(0) = m > 0, \quad R_H(0) = n > 0, \quad R_I(0) = o > 0, \\ W(0) = p > 0, \quad Y(0) = q > 0. \end{gathered} \tag{7}$$

Table 1. Description of model variables

Variable	Description
$H(t)$	Number of healthy coconut tree individuals at time t
$X(t)$	Number of infected coconut tree individuals at time t
$R_H(t)$	Number of healthy rhinoceros beetle individuals at time t
$R_I(t)$	Number of infected rhinoceros beetle individuals at time t
$W(t)$	Number of red palm weevil individuals at time t
$Y(t)$	Number of Oryctes rhinoceros nudivirus individuals at time t

2.1. Basic properties of the model

2.1.1. Positivity

From Eqs. (1) to (6), we find that

$$\left.\frac{dH}{dt}\right|_{H=0,\, X>0,\, R>0} = s \geqslant 0, \quad \left.\frac{dX}{dt}\right|_{H>0,\, X=0,\, R>0} = \frac{\alpha RH}{1+\gamma H} \geqslant 0, \quad \left.\frac{dR}{dt}\right|_{H>0,\, X>0,\, R=0} = 0. \tag{8}$$

Consequently, the solutions are positive whenever the initial conditions of the system are positive.

2.1.2. Boundedness

Let $N = H + X$, representing the total coconut tree biomass at any time t. By combining the equations of H and X we get

$$\frac{dN}{dt} = s - rX - \left(\frac{\alpha_1 RH}{1+\gamma_1 H} + \frac{\alpha_2 WH}{1+\gamma_2 H}\right), \tag{9}$$

since both terms involving R and W are non-negative, we can bound the growth rate as follows:

$$\frac{dN}{dt} \leqslant s. \tag{10}$$

Thus, the total tree biomass N is bounded by

$$\limsup_{t\to\infty} N \leqslant M := \max\{N(0),\ s\}. \tag{11}$$

Table 2. Description of model parameters [Caasia, Guerrerob, 2023; Dhivyadharshini, Senthamarai, 2024; Suganya, Senthamarai, 2022a]

Variable	Description	Values	Unit
s	Growth rate of healthy coconut trees	0.038	day^{-1}
α_1, α_2	Attack rate of rhinoceros beetles and red palm weevils on healthy trees	0.02, 0.015	day^{-1}
k_1, k_2	Death rate of infected trees due to beetles and weevils	0.01, 0.008	day^{-1}
r	Natural recovery rate of infected trees	0.03	day^{-1}
γ_1, γ_2	Growth rate of rhinoceros beetles and red palm weevils	0.04, 0.035	day^{-1}
k_R, k_W	Carrying capacities for beetle and weevil populations	500, 300	—
μ_R, μ_W	Natural death rate of beetles and weevils	0.02, 0.025	day^{-1}
β	Infection rate of rhinoceros beetles by the Oryctes virus	0.0005	day^{-1}
γ	Virus-induced mortality rate in infected beetles	0.01	day^{-1}
θ	Rate at which controlling rhinoceros beetles helps control red palm weevils	0.03	day^{-1}
ρ	Rate at which infected beetles spread the Oryctes virus	0.02	day^{-1}
η	Decay rate of the virus population	0.015	day^{-1}
δ_v	External contribution to virus growth	0.005	day^{-1}

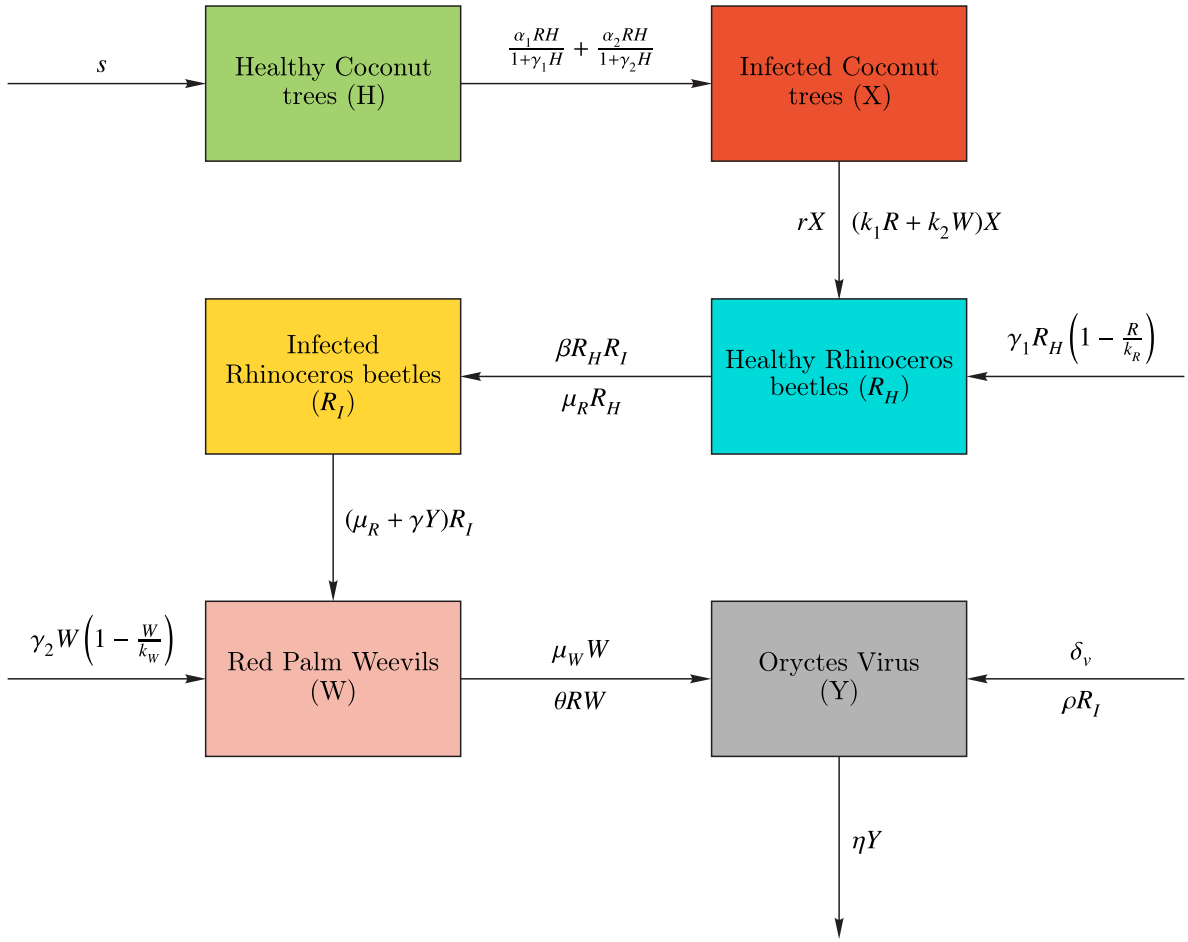

Figure 1. Model flow diagram

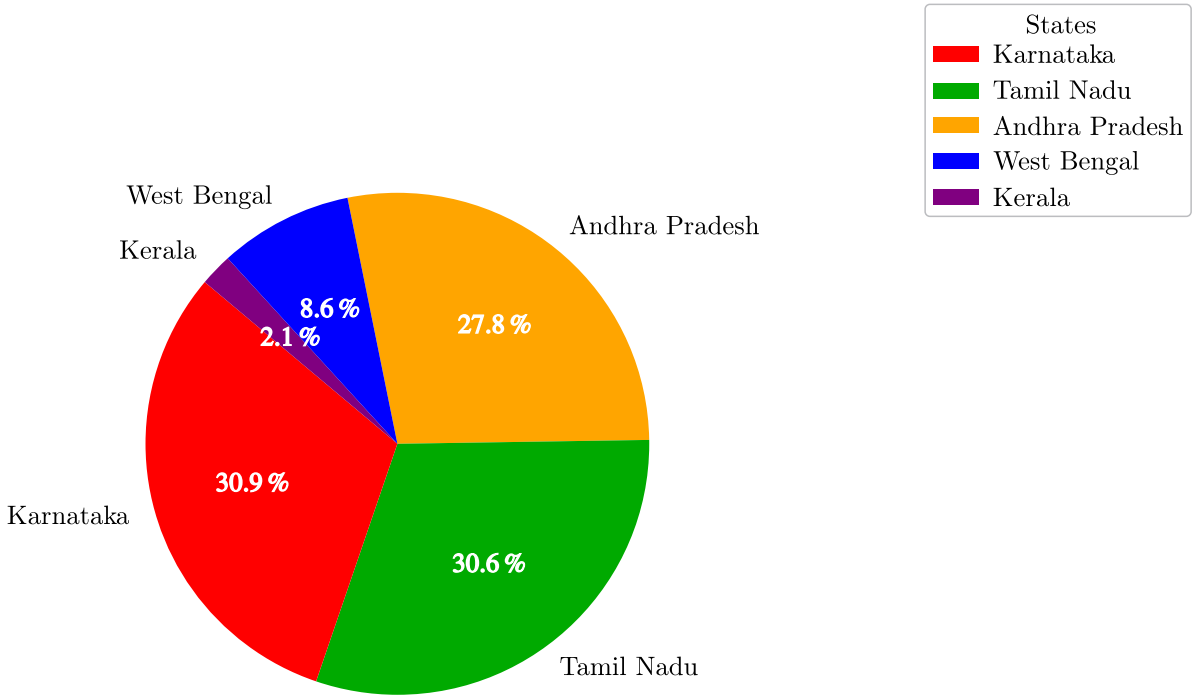

Figure 2. Top 5 coconut producing states in India (2023–2024)

From the logistic growth of the healthy rhinoceros beetle population and associated loss terms, the healthy beetle population R_H satisfies

$$\limsup_{t\to\infty} R_H \leqslant k_R. \tag{12}$$

For the infected rhinoceros beetle population R_I, since R_H is bounded and the mortality terms are non-negative, we obtain

$$\limsup_{t\to\infty} R_I \leqslant \frac{\beta K_R}{\mu_R + \gamma}. \tag{13}$$

From the red palm weevil dynamics, where the growth is logistic and the mortality includes control via beetles, we conclude

$$\limsup_{t\to\infty} W \leqslant k_W. \tag{14}$$

For the oryctes virus population Y, using boundedness of R_I and the decay term, the upper bound becomes

$$\limsup_{t\to\infty} Y \leqslant \frac{\delta_v + \rho k_R}{\eta}. \tag{15}$$

Thus, the region of attraction for the system is

$$\mathcal{D} = \left\{ (H, X, R_H, R_I, W, Y) \in \mathbb{R}^6_+ : \begin{array}{l} 0 \leqslant H + X \leqslant M, \\ 0 \leqslant R_H \leqslant k_R, \\ 0 \leqslant R_I \leqslant \dfrac{\beta k_R}{\mu_R + \gamma}, \\ 0 \leqslant W \leqslant k_W, \\ 0 \leqslant Y \leqslant \dfrac{\delta_v + \rho k_R}{\eta} \end{array} \right\}. \tag{16}$$

This region $\mathcal{D}$ is positively invariant and attracts all trajectories that start in the positive cone, thereby confirming the boundedness of all populations in the model.

3. Model analysis

3.1. Local stability of the pest free equilibrium (PFE)

At the pest-free equilibrium $E_0 = \left(s, 0, 0, 0, \frac{s}{\eta}\right)$, we analyze the matrices representing transmission and new infections. The reproduction number is then calculated using the next-generation matrix approach [Moslim et al., 2011]:

$$R_0 = \frac{\alpha_1 \eta s}{(\eta \mu_R + \gamma s)(1 + \gamma_1 s)}.$$

Lemma 1. *The PFE E_0 of the model equations* (1)–(6) *is locally asymptotically stable if $R_0 < 1$ and unstable if $R_0 > 1$.*

Lemma 1 implies that, for $R_0 < 1$, a small influx of infectious individuals will not lead to a large outbreak of the disease. To ensure that disease elimination is independent of the initial sizes of sub-populations, however it is necessary to show that the PFE is globally asymptotically stable if $R_0 < 1$. This is explored below.

3.2. Global stability of the pest free equilibrium

Theorem 1. *The PFE of the model equations* (1)–(6)*, given by Eq.* (3)*, is globally asymptotically stable whenever $R_0 \leqslant 1$.*

Proof. A comparison theorem will be used for the proof. The equations for the infected components of the model equations (2), (4) and (6) can be simplified as follows, where N^* is the total population

$$\begin{bmatrix} \frac{dX}{dt} \\ \frac{dR_I}{dt} \\ \frac{dV}{dt} \end{bmatrix} = \left(\frac{H}{N^*}\right) F \begin{bmatrix} X \\ R_I \\ Y \end{bmatrix} - V \begin{bmatrix} X \\ R_I \\ Y \end{bmatrix} =$$

$$= (F - V) \begin{bmatrix} X \\ R_I \\ Y \end{bmatrix} - \left(1 - \frac{H}{N^*}\right) F \begin{bmatrix} X \\ R_I \\ Y \end{bmatrix} \leqslant \tag{17}$$

$$\leqslant (F - V) \begin{bmatrix} X \\ R_I \\ Y \end{bmatrix}, \tag{18}$$

with F and V defined as earlier.

Lemma 1 confirms that the PFE is locally asymptotically stable for $R_0 < 1$, or equivalently, when $\rho\left(FV^{-1}\right) < 1$. This condition implies that all eigenvalues of $F - V$ have negative real parts, as shown in [Van den Driessche, Watmough, 2002]. Thus, the linearized form of Eq. (18) satisfies a differential inequality, and by a standard comparison theorem, it follows that

$$(X, R_I, Y) \to \left(0, 0, \frac{s}{\eta}\right) \quad \text{as } t \to \infty. \tag{19}$$

Substituting Eq. (19) in the model equations (1)–(6) gives

$$(H, R_H, W) \to (s, 0, 0) \quad \text{as } t \to \infty. \tag{20}$$

Therefore,

$$(H, X, R_H, R_I, W, Y) \to \left(s, 0, 0, 0, 0, \frac{s}{\eta}\right) \quad \text{as } t \to \infty. \tag{21}$$

Thus, the PFE E_0 is globally asymptotically stable whenever $R_0 \leqslant 1$. This implies, from an epidemiological perspective, that the pest population can be eradicated if the basic reproduction number R_0 is reduced below unity and kept there. Hence, the condition $R_0 < 1$ serves as both a necessary and sufficient criterion for disease elimination.

3.3. Existence and Global Stability of the endemic equilibrium

In this section, the existence of endemic equilibria and global stability of the model equations (1)–(6) will be discussed.

3.3.1. Existence of endemic equilibrium

Let $E^* = (H^*, X^*, R_H^*, R_I^*, W^*, Y^*)$ denote an arbitrary endemic equilibrium of the model equations (1)–(6) so that where,

$$X^* = \frac{\frac{\alpha_1 R_H^* H^*}{1+\gamma_1 H^*} + \frac{\alpha_2 R_H^* H^*}{1+\gamma_2 H^*}}{k_1 R^* + k_2 W^* + r}, \quad R_H^* = k_R\left(1 - \frac{\mu_R + \beta R_I^*}{\gamma_1}\right), \quad R_I^* = \frac{\beta R_H^* R_I^*}{\mu_R + \gamma Y^*},$$
$$W^* = k_W\left(1 - \frac{\mu_W + \theta R^*}{\gamma_2}\right), \quad Y^* = \frac{\delta_v + \rho R_I^*}{\eta}.$$

Theorem 2. *The endemic equilibrium of the system of equations* (1)–(6) *is globally asymptotically stable in* Ω *whenever* $R_0 > 1$.

Proof. Let the endemic equilibrium of the system of equations (1)–(6) be denoted by $E^* = (H^*, X^*, R_H^*, R_I^*, W^*, Y^*)$ and let $R_0 > 1$ so that E^* exists. Consider the following non-linear Goh–Volterra type Lyapunov function:

$$V = H - H^* - H^* \ln\left(\frac{H}{H^*}\right) + X - X^* - X^* \ln\left(\frac{X}{X^*}\right) + R_H - R_H^* - R_H^* \ln\left(\frac{R_H}{R_H^*}\right) +$$
$$+ R_I - R_I^* - R_I^* \ln\left(\frac{R_I}{R_I^*}\right) + W - W^* - W^* \ln\left(\frac{W}{W^*}\right) + Y - Y^* - Y^* \ln\left(\frac{Y}{Y^*}\right),$$

with the Lyapunov derivative

$$\dot{V} = \left(1 - \frac{H^*}{H}\right)\dot{H} + \left(1 - \frac{X^*}{X}\right)\dot{X} + \left(1 - \frac{R_H^*}{R_H}\right)\dot{R}_H + \left(1 - \frac{R_I^*}{R_I}\right)\dot{R}_I + \left(1 - \frac{W^*}{W}\right)\dot{W} + \left(1 - \frac{Y^*}{Y}\right)\dot{Y},$$

where the upper dot represents the differentiation with respect to time. Putting the appropriate equations of the system (1)–(6) into the above, we have

$$\begin{aligned}\dot{V} = &\left(1-\frac{H^*}{H}\right)\left[s-\left(\frac{\alpha_1 RH}{1+\gamma_1 H}+\frac{\alpha_2 WH}{1+\gamma_2 H}\right)\right]+\\ &+\left(1-\frac{X^*}{X}\right)\left[\left(\frac{\alpha_1 RH}{1+\gamma_1 H}+\frac{\alpha_2 WH}{1+\gamma_2 H}\right)-(k_1R+k_2W)X-rX\right]+\\ &+\left(1-\frac{R_H^*}{R_H}\right)\left[\gamma_1 R_H\left(1-\frac{R}{k_R}\right)-\mu_R R_H-\beta R_H R_I\right]+\left(1-\frac{R_I^*}{R_I}\right)\left[\beta R_H R_I-\left(\mu_R+\gamma V\right)R_I\right]+\\ &+\left(1-\frac{W^*}{W}\right)\left[\gamma_2 W\left(1-\frac{W}{k_W}\right)-\mu_W W-\theta R_H W\right]+\left(1-\frac{Y^*}{Y}\right)[\delta_v+\rho R_I-\eta Y]. \end{aligned} \tag{22}$$

Now, at steady-states,

$$\begin{aligned} s &= \frac{\alpha_1 R^* H^*}{1+\gamma_1 H^*}+\frac{\alpha_2 W^* H^*}{1+\gamma_2 H^*},\\ \frac{\alpha_1 R^* H^*}{1+\gamma_1 H^*}+\frac{\alpha_2 W^* H^*}{1+\gamma_2 H^*} &= (k_1R^*+k_2W^*)X^*+rX^*,\\ \gamma_1 R_H^*\left(1-\frac{R^*}{k_R}\right) &= \mu_R R_H^*+\beta R_H^* R_I^*,\\ \beta R_H^* R_I^* &= (\mu_R+\gamma Y^*)R_I^*,\\ \gamma_2 W^*\left(1-\frac{W^*}{k_W}\right) &= \mu_W W^*+\theta R_H^* W^*,\\ \delta_v+\rho R_I^* &= \eta Y^*. \end{aligned} \tag{23}$$

After substituting all steady-state conditions into the Lyapunov derivatives, we have $\dot{V}=0$ for $R_0>1$. Hence, V is a Lyapunov function in Ω and it follows by the Lasalle invariance principle [Hale, 1969] that every solution to the equations of the system (1)–(6) with an initial condition in $\Omega\setminus\Omega_0$ approaches the associated unique endemic equilibrium E^* of the model as $t\to\infty$ for $R_0>1$.

4. Sensitivity analysis

This section analyzes how variations in parameter values influence the basic reproduction number R_0. Identifying the most sensitive parameters is essential, as they may act as critical thresholds for effective disease control. Below are the algebraic expressions for the sensitivity indices of R_0 with respect to the parameters $s,\alpha_1,\alpha_2,k_1,k_2,r,\gamma_1,\gamma_2,k_R,k_W,\mu_R,\mu_W,\beta,\gamma,\theta,\rho,\eta,\delta_v$:

$$\frac{\partial R_0}{\partial s}=\alpha_1\eta\left(\frac{\eta\mu_R-\gamma\gamma_1 s^2}{[(\eta\mu_R+\gamma s)(1+\gamma_1 s)]^2}\right),\quad \frac{\partial R_0}{\partial \alpha_1}=\frac{\eta s}{(\eta\mu_R+\gamma s)(1+\gamma_1 s)},\quad \frac{\partial R_0}{\partial \alpha_2}=0,$$
$$\frac{\partial R_0}{\partial k_1}=0,\quad \frac{\partial R_0}{\partial k_2}=0,\quad \frac{\partial R_0}{\partial r}=0,\quad \frac{\partial R_0}{\partial \gamma_1}=-\alpha_1\eta s^2\frac{1}{(\eta\mu_R+\gamma s)(1+\gamma_1 s)^2},\quad \frac{\partial R_0}{\partial \gamma_2}=0,$$
$$\frac{\partial R_0}{\partial k_R}=0,\quad \frac{\partial R_0}{\partial k_W}=0,\quad \frac{\partial R_0}{\partial \mu_R}=-\frac{\alpha_1\eta^2 s}{(\eta\mu_R+\gamma s)(1+\gamma_1 s)},\quad \frac{\partial R_0}{\partial \mu_W}=0,\quad \frac{\partial R_0}{\partial \beta}=0,$$
$$\frac{\partial R_0}{\partial \gamma}=-\frac{\alpha_1\eta s^2}{(\eta\mu_R+\gamma s)^2(1+\gamma_1 s)},\quad \frac{\partial R_0}{\partial \theta}=0,\quad \frac{\partial R_0}{\partial \rho}=0,\quad \frac{\partial R_0}{\partial \eta}=\frac{\alpha_2\gamma s^2}{(\eta\mu_R+\gamma s)(1+\gamma_1 s)},\quad \frac{\partial R_0}{\partial \delta_v}=0.$$

In conclusion, the partial derivatives with respect to parameters s, α_1, η are positive, indicating that the basic reproduction number R_0 increases as any of these parameters increase. The elasticity is evaluated

based on the proportional change in R_0 resulting from a proportional change in each parameter. We have

$$E_s = \frac{s}{R_0}\frac{\partial R_0}{\partial s} = 0.44, \quad E_{\alpha_1} = \frac{\alpha_1}{R_0}\frac{\partial R_0}{\partial \alpha_1} = 1.00, \quad E_\eta = \frac{\eta}{R_0}\frac{\partial R_0}{\partial \eta} = 0.56.$$

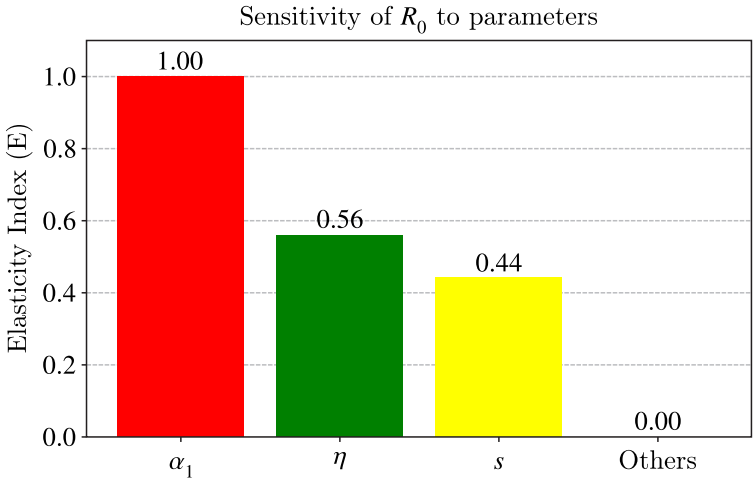

Figure 3. Elasticity analysis of R_0 with respect to model parameters

The expressions clearly show that E_s, E_{α_1}, E_η are all positive, indicating that an increase in the parameters s, α_1, η leads to an increase in the basic reproduction number R_0. Even slight changes in these parameters can produce significant shifts in R_0, emphasizing the need to identify and manage highly sensitive parameters with care.

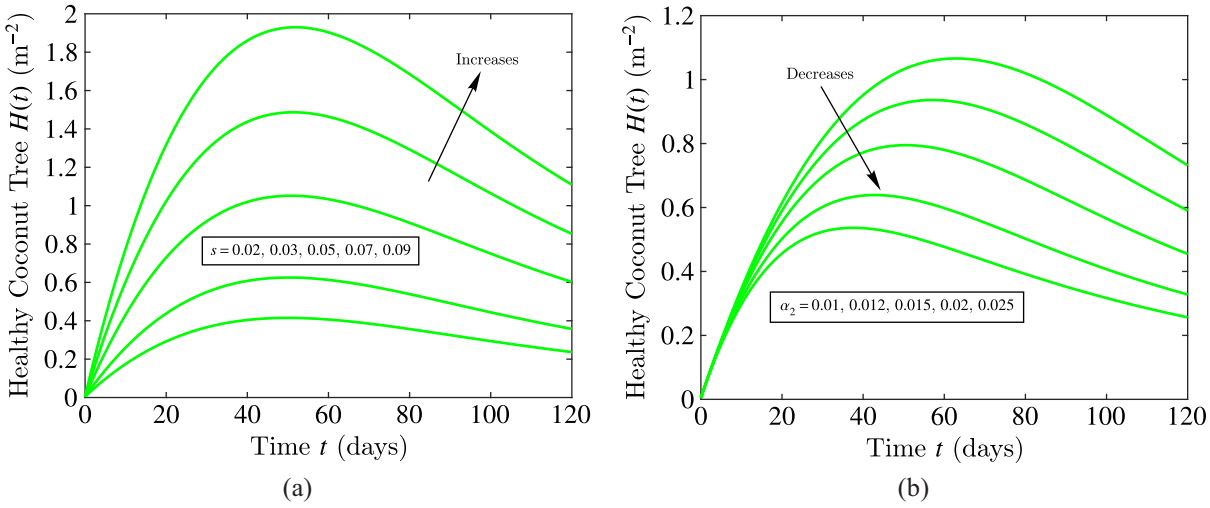

Figure 4. Profiles of the healthy tree density $H(t)$ versus time (120 days): (a) for different values of growth rate of healthy coconut trees s; (b) for different values of attack rate of rhinoceros beetles on healthy trees α_2 with other parameters as given in Table 2

5. Results and discussion

To perform the numerical study, reference values were assigned to each parameter. We assume the initial conditions to be $H(0) = 0.005$, $X(0) = 0.0007$, $R_H(0) = 0.001$, $R_I(0) = 0.0001$, $W(0) = 2$,

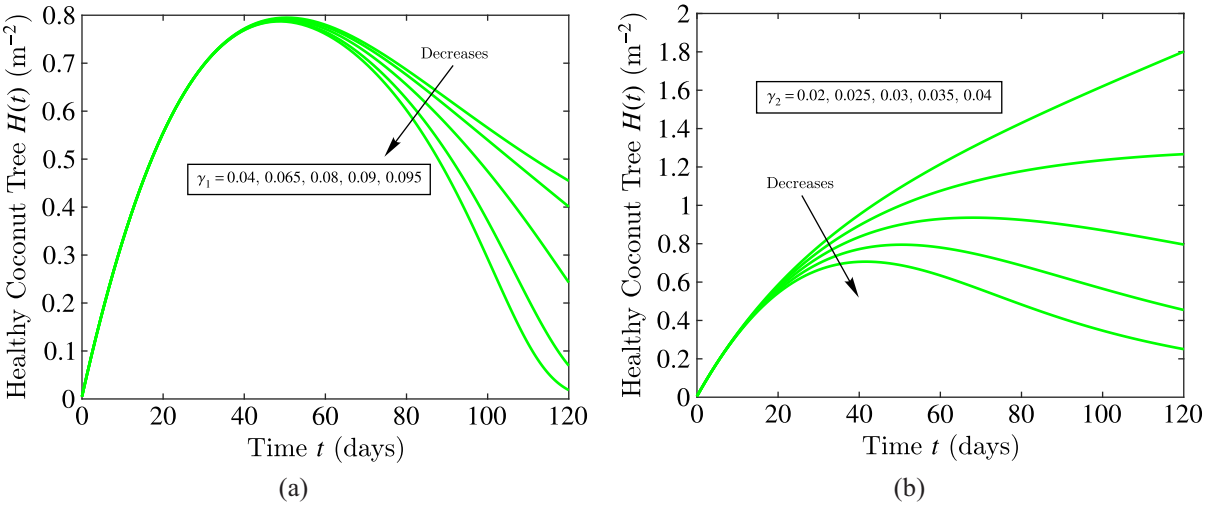

Figure 5. Profiles of the healthy tree density $H(t)$ versus time (120 days): (a) for different values of growth rate of rhinoceros beetles γ_1; (b) for different values of growth rate of weevils γ_2 with other parameters as given in Table 2

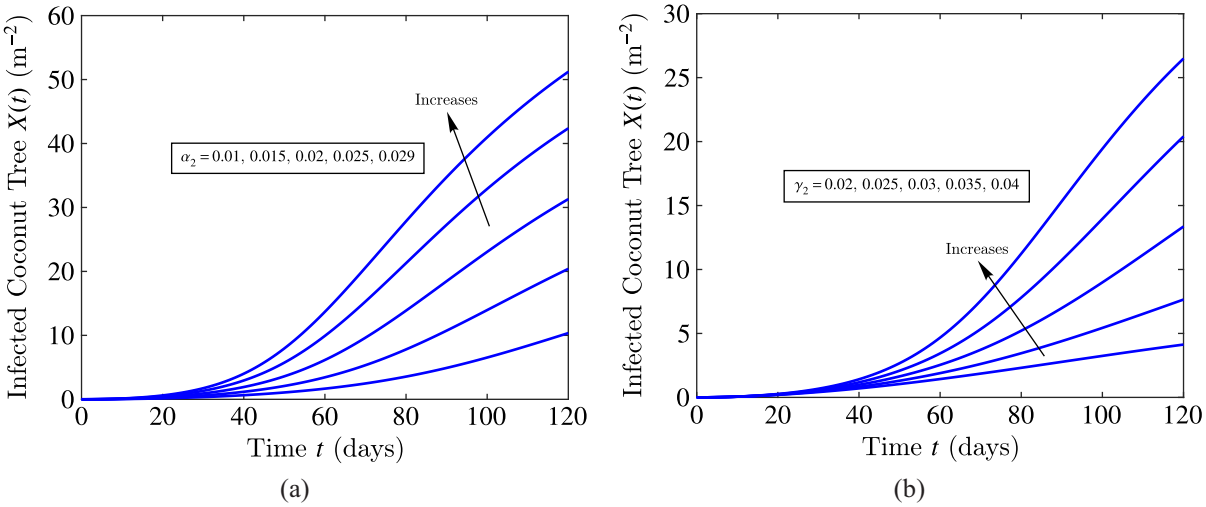

Figure 6. Profiles of the infected tree density $X(t)$ versus time (120 days): (a) for different values of attack rate of rhinoceros beetles on healthy trees α_2; (b) for different values of growth rate of red palm weevils γ_2 with other parameters as given in Table 2

$Y(0) = 0$. Parameter values were selected based on the findings and approaches described in [Caasia, Guerrerob, 2023; Dhivyadharshini, Senthamarai, 2024; Suganya, Senthamarai, 2022a]. Table 1 shows the description of model variables. Table 2 lists all the parameter values used and the numerical simulations were performed using MATLAB.

Figure 1 shows the model flow diagram. Figure 2 shows Top 5 coconut producing states in India (2023–2024) source given in ministry of agriculture and farmers welfare, Government of India. Figure 3 shows the Elasticity analysis of R_0 with respect to model parameters. Figure 4, *a* interprets that the growth rate s increases the healthy tree density, while Fig. 4, *b* shows that the attack rate of rhinoceros beetles α_2 decreases it. Figure 5, *a* interprets that the growth rate of rhinoceros beetles γ_1 reduces healthy tree density, and Fig. 5, *b* shows a similar effect due to the red palm weevil growth rate γ_2. Figure 6, *a* interprets that the attack rate of rhinoceros beetles on healthy trees α_2 increases the

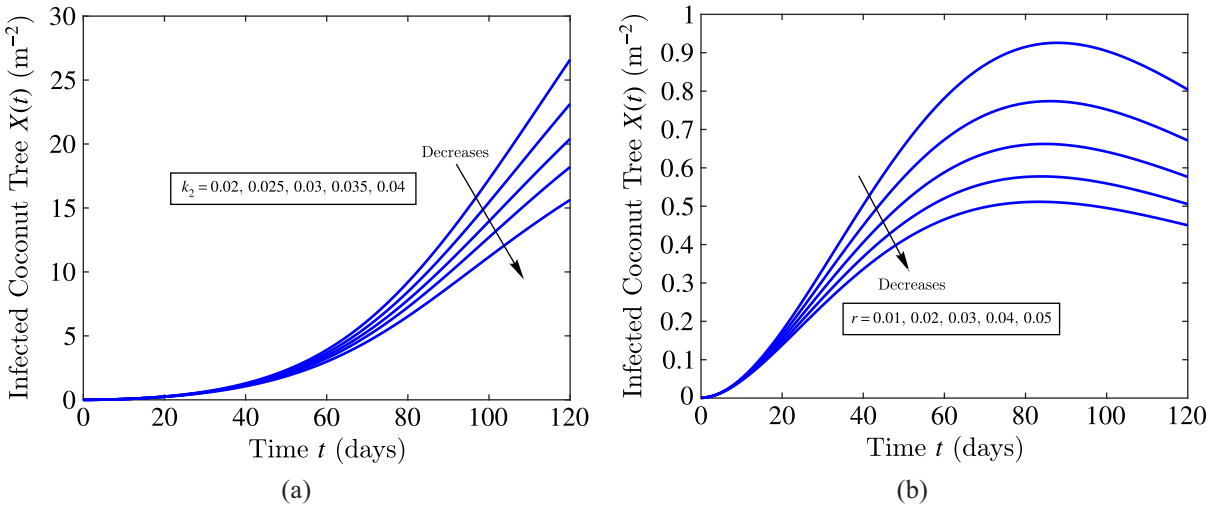

Figure 7. Profiles of the infected tree density $X(t)$ versus time (120 days): (a) for different values of death rate of infected trees due to weevils k_2; (b) for different values of natural recovery rate of infected trees r with other parameters as given in Table 2

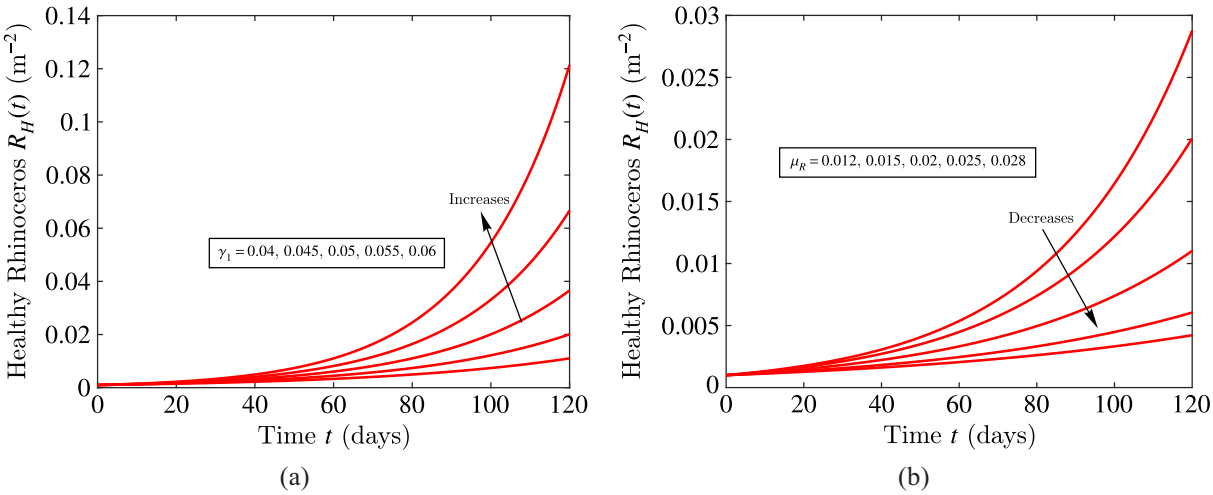

Figure 8. Profiles of the healthy rhinoceros beetles density R_H versus time (120 days): (a) for different values of growth rate of rhinoceros beetles γ_1; (b) for different values of natural death rate of beetles μ_R with other parameters as given in Table 2

infected tree density and Fig. 6, *b* growth rate of red palm weevils γ_2 contributes to this increase as well. Figure 7, *a* interprets that the death rate of infected trees due to weevils k_2 decreases the infected tree density, while Fig. 7, *b* shows that the natural recovery rate of infected trees r has a similar decreasing effect. Figure 8, *a* interprets that the growth rate of rhinoceros beetles γ_1 increases the healthy rhinoceros beetles density, whereas Fig. 8, *b* shows that the natural death rate of weevils μ_R reduces it. Figure 9, *a* interprets that the natural death rate of weevils μ_R reduces the infected beetle density, and Fig. 9, *b* shows that the virus induced mortality rate γ leads to a similar decline. Figure 10 interprets that the infection rate of rhinoceros beetles by the oryctes virus β reduces the infected rhinoceros beetles density. Figure 11, *a* interprets that the growth rate of red palm weevils γ_2 increases Fig. 11, *b* carrying capacities for weevil populations k_W also increases the red weevil density. Figure 12, *a* interprets that the natural death rate of weevils μ_W reduces OrNV density, and Fig. 12, *b* shows the rate at which controlling rhinoceros beetles helps control red palm weevils θ also contributes

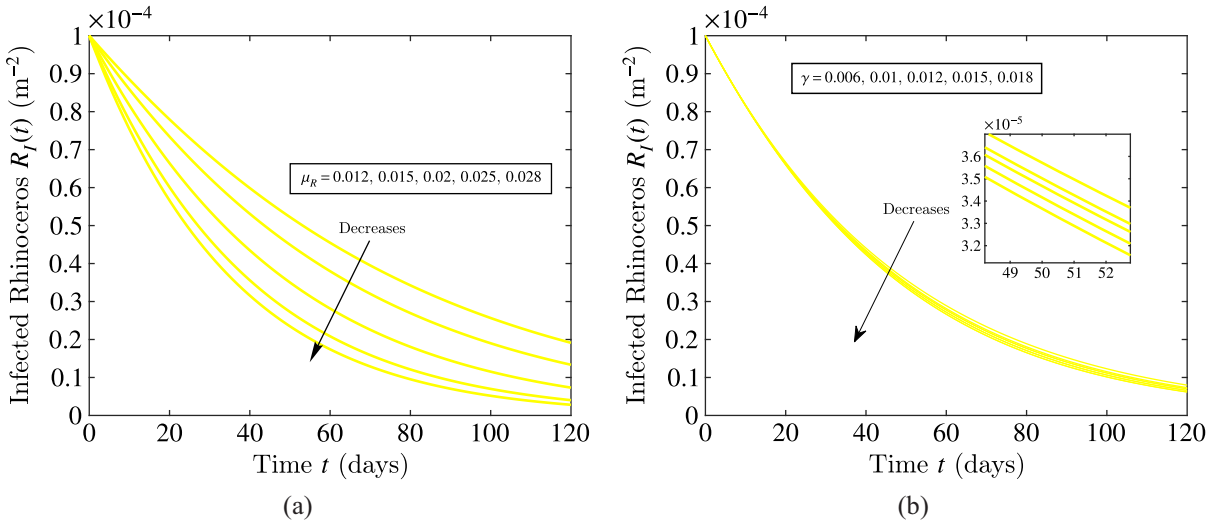

Figure 9. Profiles of the infected rhinoceros beetles $R_I(t)$ versus time (120 days): (a) for different values of natural death rate of beetles μ_R; (b) for different values of virus induced mortality rate in infected beetles γ with other parameters as given in Table 2

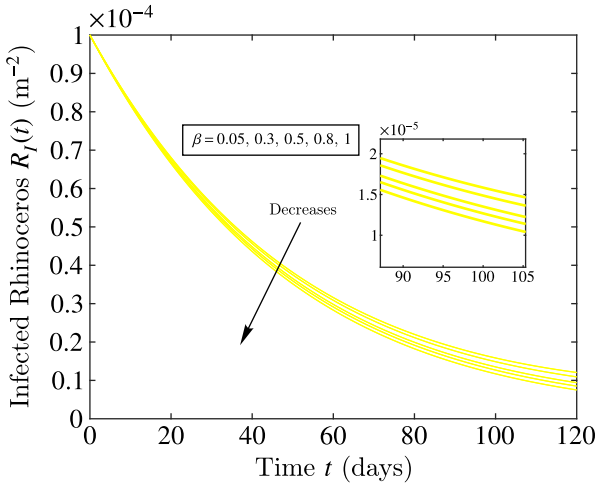

Figure 10. Profiles of the infected rhinoceros beetles $R_I(t)$ versus time (120 days) for different values of infection rate of rhinoceros beetles by the oryctes virus β with other parameters as given in Table 2

to this reduction. Figure 13, *a* interprets that the decay rate of the virus population η decreases, and Fig. 13, *b* shows that the external contribution to virus growth δ_v increases the OrNV density.

6. Conclusion

This study highlights the significant role of CRB management in indirectly reducing red palm weevil populations in coconut plantations. Through the construction and analysis of a detailed mathematical model involving healthy and infected trees, pest species, and a biological control agent (OrNV), we demonstrate that targeted intervention against CRBs can effectively suppress red palm weevil infestations. The results are validated through numerical simulations and graphical analyses, which emphasize the importance of the interspecific interaction parameter θ, representing the rate at which controlling CRBs helps control red palm weevils. It is clearly shown that enhancing θ leads to a notable decline in red palm weevil populations. These findings confirm that CRB control not

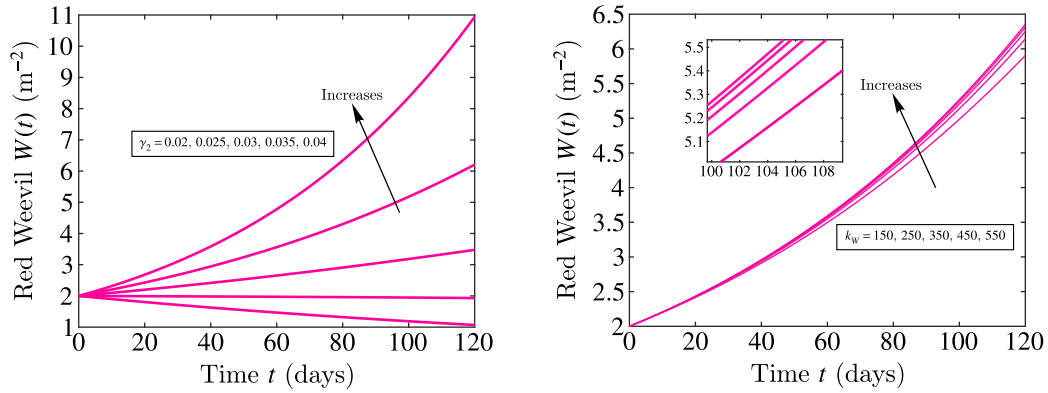

Figure 11. Profiles of the red weevil density $W(t)$ versus time (120 days): (a) for different values of growth rate of red palm weevils γ_2; (b) for different values of carrying capacities for weevil populations k_W with other parameters as given in Table 2

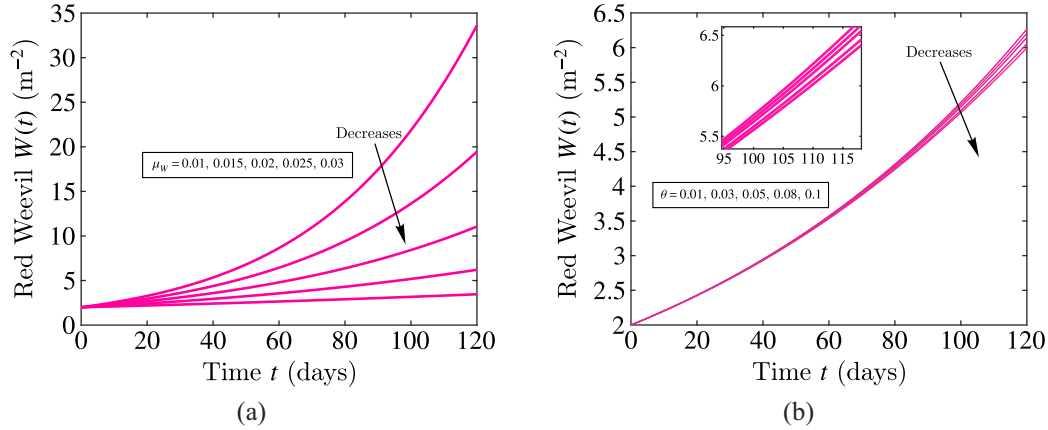

Figure 12. Profiles of the red weevil density $W(t)$ versus time (120 days): (a) for different values of natural death rate of weevils μ_W; (b) for different values of rate at which controlling rhinoceros beetles helps control red palm weevils θ with other parameters as given in Table 2

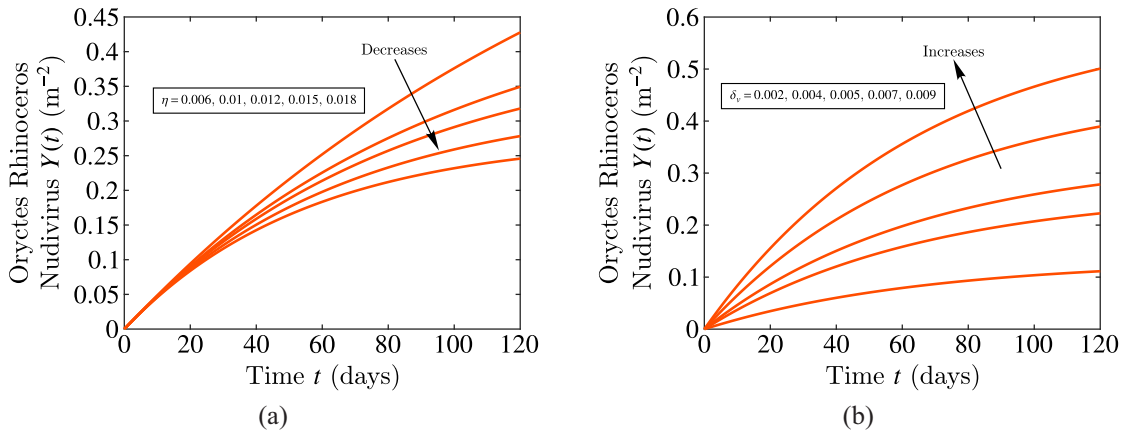

Figure 13. Profiles of the OrNV density $Y(t)$ versus time (120 days): (a) for different values of decay rate of the virus population η; (b) for different values of external contribution to virus growth δ_v with other parameters as given in Table 2

only reduces their own numbers but also indirectly influences red palm weevil dynamics, supporting a holistic and ecologically responsible approach to pest management. Overall, the model provides a strong scientific basis for designing robust control strategies, offering practical insights into pest interactions and sustainable protection of coconut crops.

Acknowledgements

We sincerely thank the reviewers for their valuable comments, which were of great help in revising the manuscript. It is our pleasure to thank the College of Engineering and Technology, SRM IST for its valuable support and constant encouragement.

Conflict of interest

The authors declare that there is no conflict of interest.

References

Allen L. J., Brauer F., Van den Driessche P., Wu J. Mathematical epidemiology. — Berlin: Springer, 2019.

Barlow H. S., Chew P. S. The rhinoceros beetle Oryctes rhinoceros in young oil palms replanted after rubber on some estates in Western Malaysia // Proceedings of the Malaysian Crop Protection Conference. — 1970.

Bedford G. O. Biology and management of palm dynastid beetles: Recent advances // Annual Review of Entomology. — 2013. — Vol. 58. — P. 353–372.

Bedford G. O. Biology, ecology and control of palm rhinoceros beetles // Annual Review of Entomology. — 1980. — Vol. 25. — P. 309–339.

Caasia J. A. S., Guerrerob A. L. A mathematical model of invasion and control of coconut rhinoceros beetle Oryctes rhinoceros (L.) in Guam // Journal of theoretical biology. — 2023. — Vol. 570. — 111525.

Dayrit F. M., Mary T. N. Potential of coconut oil and its derivatives as effective and safe antiviral agents against the novel coronavirus // Indian Coconut Journal. — 2020. — Vol. 62. — P. 21–23.

Dhivyadharshini B., Senthamarai R. Mathematical analysis of a non linear prey predator system: analytical approach by HPM // AIP Conference Proceedings. — 2022. — Vol. 2516.

Dhivyadharshini B., Senthamarai R. Modeling rugose spiraling whitefly infestation on coconut trees using delay differential equations: analysis via HPM // European Journal of Pure and Applied Mathematics. — 2024. — Vol. 17, No. 3. — P. 1908–1936.

Diekmann O., Heesterbeek J. A. P., Metz J. A. J. On the definition and the computation of the basic reproduction ratio R_0 in models for infectious diseases in heterogeneous populations // Journal of Mathematical Biology. — 1990. — Vol. 28, No. 4. — P. 365–382.

Hale J. K. Ordinary differential equations. — New York: John Wiley and Sons, 1969.

Hochberg M. E., Waage J. K. A model for the biological control of Oryctes Rhinoceros (Coleoptera: Scarabaeidae) by means of pathogens // Journal of Applied Ecology. — 1991. — Vol. 28. — P. 514–531.

Ijinu T. P., Anish N., Shiju H., George V., Pushpangadan P. Home gardens for nutritional and primary health security of rural poor of South Kerala // Indian Journal of Traditional Knowledge. — 2011. — Vol. 10, No. 3. — P. 413–428.

Jayasekhar S., Chandran K. P., Thamban C., Muralidharan K. Coconut sector in India experiencing a new regime of trade and policy environment: A critical analysis // Journal of Plantation Crops. — 2019. — Vol. 47, No. 1. — P. 48–54.

Marshall S. D. G., Moore A., Vaqalo M., Noble A., Jackson T. A. A new haplotype of the coconut rhinoceros beetle, Oryctes rhinoceros, has escaped biological control by Oryctes rhinoceros nudivirus and is invading Pacific islands // Journal of Invertebrate Pathology. — 2017. — P. 127–134.

Moslim R., Kamarudin N., Ghani I., Wahid M., Jackson T., Tey C. C., Ahdly A. M. Molecular approaches in the assessment of oryctes rhinoceros virus for the control of rhinoceros beetle in oil palm plantations // Journal of Oil Palm Research. — 2011. — Vol. 23. — P. 1096–1109.

Nadanasabapathy S., Kumar R. Physico-chemical constituents of tender coconut (Cocos nucifera) water // The Indian Journal of Agricultural Sciences. — 2013. — Vol. 69. — P. 750–751.

Nair C. P. R., Sathiamma B., Mohan C., Gopal M. Newer approaches in the integrated pest management in coconut // Indian Coconut Journal. — 1998.

Nirula K. K., Antony J., Menon K. P. V. The red palm weevil and its control // Proceedings of the 40th Session, Indian Science Congress. — 1953. — P. 147–148.

Secretariat of the Pacific Community. An emerging biotype of Coconut Rhinoceros Beetle Discovered in the Pacific // Pest Alert. — 2015. — Vol. 51.

Sreejith C. C., Muraleedharan C., Arun P. Life cycle assessment of producer gas derived from coconut shell and its comparison with coal gas: An Indian perspective // International Journal of Energy Environment Engineering. — 2013. — Vol. 4. — P. 1–22.

Suganya G., Senthamarai R. Analytical approximation of a nonlinear model for pest control in coconut trees by the homotopy analysis method // Computer Research and Modeling. — 2022a. — Vol. 14, No. 5. — P. 1093–1106.

Suganya G., Senthamarai R. Impact of awareness on the dynamics of pest control in coconut trees — A mathematical model // Engineering Letters. — 2022b. — Vol. 30, No. 4.

Suganya G., Senthamarai R. Mathematical modeling and analysis of the effect of the rugose spiraling whitefly on coconut trees // AIMS Mathematics. — 2022c. — Vol. 7, No. 7. — P. 13053–13073.

Umana R. A., Omame A., Inyama S. C. Deterministic and stochastic models of the dynamics of drug resistant tuberculosis // FUTO Journal Series (FUTOJNLS). — 2016. — Vol. 2, No. 2. — P. 173–194.

Van den Driessche P., Watmough J. Reproduction numbers and sub-threshold endemic equilibria for compartmental models of disease transmission // Mathematical Biosciences. — 2002. — Vol. 180. — P. 29–48.

Varghese A., Jacob J. A study of physical and mechanical properties of the Indian coconut for efficient dehusking // Journal of Natural Fibers. — 2017. — Vol. 14, No. 3. — P. 390–399.

Winotai A. Integrated pest management of important insect pests of coconut // Cord. — 2014. — Vol. 30, No. 1. — P. 18–36.